physica status solidi b
www.pss-b.com

Structural and Electrical Characterization of Solution-Deposited β-Ga_2O_3:Al

Valentine W. Muramba, Abdulraoof I. A. Ali, and Jacqueline M. Nel*

The wide bandgap oxide semiconductor thin films are synthesized using tetrahydroxogallate (III) ammonium {$NH_4Ga(OH)_4$} precursor at a concentration of 10 at% Ga and varying amounts of hydrated aluminum nitrate between 0.6 and 3.2 at%. Thin films of β-Ga_2O_3:Al are synthesized by spin coating and spray pyrolysis with postannealing in nitrogen ambient at 930 °C. The structural properties of the thin films are investigated using XRD and Raman spectroscopy, while the electrical characteristics are determined using 4-point probe, current–voltage (*I–V*), and capacitance–voltage (*C–V*) measurements with Ti/Al/Ni/Au Ohmic contacts and Pd/Au Schottky contacts. The β-Ga_2O_3 with 2.2 at% Al is found to be the optimal concentration in this study, resulting in ideality factors of 1.10 and 1.09, saturation currents of 3.17×10^{-6} and 3.10×10^{-6} A, Schottky barrier heights of 0.73 and 0.88 eV, and series resistances of 948 and 955 Ω, for the spin-coated and pyrolytically sprayed samples respectively.

1. Introduction

Among the wide bandgap semiconductors, gallium oxide is attracting a lot of research in the semiconductor oxide field for optoelectronic applications due to its high breakdown voltage, high thermal stability, low-ON-state resistance, low leakage current, and to some extent, good thermal conductivity.[1–4] Many of the recent studies show that doping Ga_2O_3 improved the structural, optical, and electrical properties.[5–9] Doping of β-Ga_2O_3 with metals other than the common group of four elements (i.e., Si, Ge, and Sn) tends to improve these properties further. It was also established that the structure of the material, annealing temperature, and ambient of annealing contribute to the electrical properties.[10–12] It is therefore important to investigate the effect of doping and postannealing on the material structure using XRD and Raman spectroscopy.

Studies showed that aluminum doping of β-Ga_2O_3 enhanced properties of this oxide subject to the precursor solution for synthesizing the oxide, the type of substrate upon which the oxide is deposited, film thickness, crystallinity, and free-charge-carrier concentration. Solution deposition is easy to upscale and low cost. Aluminum doping also creates beta-phase in-and-out plane crystallization qualities of the oxide.[6,7,9] The dopant concentration of aluminum in the range of 3.2% Al to 9.6% Al improved the conductivity of β-Ga_2O_3 as it enhanced oxygen vacancies, which was more evident on postanneling in argon other than air,[9] but no study has been carried out to optimize this dopant concentration. Doping of β-Ga_2O_3 with aluminum has also been found to lead to the forming of oxygen interstitial defects, and when deposited on silicon, the film conductivity was shown to improve.[7,8] The aluminum doping has also resulted in an increase in the bandgap and enhances the material's thermal stability, making it suitable for high-power electronic applications and UV photodetectors.[7,8]

This study was therefore carried out with the aim of optimizing the aluminum concentration in β-Ga_2O_3 by investigating dopant in the range of 0 at% Al to 3.2 at% Al with a novel precursor solution of $NH_4Ga(OH)_4$ deposited on n-type silicon substrate while comparing solution deposition techniques of spray pyrolysis and spin coating.

In a previous study, the authors have shown that a Ga concentration of 10 at% in tetrahydroxogallate (III) ammonium precursor was optimal in the synthesis and characterization of undoped β-Ga_2O_3 thin films prepared by spin coating and spray pyrolysis.[1] This has been the starting point for the doping of β-Ga_2O_3 with Al in this study to achieve an improved β-Ga_2O_3 for electrical applications. The chemical solution deposition techniques using spin coating and spray pyrolysis were chosen since they are vacuum-free and relatively cheap compared to techniques such as sputtering, physical and chemical vapor deposition, atomic layer deposition, and thermal vapor deposition.[13] The comparison between the two chosen techniques was considered to ascertain the viability of the techniques for future research using these techniques in various applications.

V. W. Muramba, A. I. A. Ali, J. M. Nel
Department of Physics
University of Pretoria
Private bag X20, Hatfield 0028, South Africa
E-mail: u19401613@tuks.co.za

V. W. Muramba
Department of Mathematics and Physics
Technical University of Mombasa
P.O. Box, 90420-80100, Mombasa 80100, Kenya

A. I. A. Ali
Faculty of Education
University of Elimam Elmahdi
Kosti, White Nile, Sudan

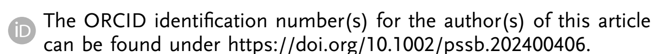
The ORCID identification number(s) for the author(s) of this article can be found under https://doi.org/10.1002/pssb.202400406.

© 2024 The Author(s). physica status solidi (b) basic solid state physics published by Wiley-VCH GmbH. This is an open access article under the terms of the Creative Commons Attribution-NonCommercial-NoDerivs License, which permits use and distribution in any medium, provided the original work is properly cited, the use is non-commercial and no modifications or adaptations are made.

DOI: 10.1002/pssb.202400406

 © 2024 The Author(s). physica status solidi (b) basic solid state physics published by Wiley-VCH GmbH

A diode is one of the major components necessary in electronic equipment. It mainly serves as a rectifier in circuits in switched-mode power supplies, solar cell circuit protection, and prevention of transistor saturation, since their low forward voltage and fast recovery times lead to increased efficiency of the device.[14] Unlike common diodes (which have a voltage drop of 0.6–0.7 V), Schottky barrier diodes (with a voltage drop of 0.1–0.2 V) consume less power and tend to be more thermally efficient at dissipating heat in high-power applications. They therefore offer fast switching action and have a low forward voltage drop.[15]

One of the factors considered in making Schottky barrier diodes is the ideality factor (n) as this is used to indicate the type of charge carrier recombination that is occurring inside the diode and is also used to identify the dominant form of recombination particularly in solar cells, and guide future development.[16] Most common diodes with reported ideality factor are made from gallium arsenide ($n = 2.45$), germanium ($n = 1.4$), and silicon ($n = 1.1$). The most recent that is attracting a lot of research are Schottky barrier diodes made from gallium oxide ($n = 1.02$) as it has the advantage over the others for being able to withstand high temperatures in high power applications.[16,17]

One of the factors that affect the efficiency of the diode is the type of electrode contact as this affects charge transport in and out of the diode.[15] In the previous studies, the electrical properties of Al-doped β-Ga_2O_3 were explored by considering resistivity, conductivity, and metal contact. The *I–V* and *C–V* characteristics were used to determine the effectiveness of the electrode contacts in terms of the properties of the diode. The electrode contacts were made with three-layer metal stacks for Ohmic contacts[14–17] and the results were not ideal for β-Ga_2O_3 based diodes.[14,15,18] In previous research, a systematic optimization study of multilayer metal stacks for Ohmic and Schottky contacts with different metals on various orientations of β-Ga_2O_3 and precursor concentration was still lacking. Metal contacts with lower leakage current to sustain large breakdown voltage were required which led to the current study research. For the purpose of electronic application of β-Ga_2O_3 and as a novelty of this research, four-layer metal stacks were investigated with metals chosen based on previous studies and their low work functions, high melting temperatures, strong electron affinity, and their formation of stable oxides.[15,19]

2. Experimental Section

2.1. Sample Preparation

The Al-doped β-Ga_2O_3 samples were prepared under the same conditions mentioned in our previous study of undoped β-Ga_2O_3 where the optimum precursor concentration of tetrahydroxogallate ammonium was determined to be 10 at% Ga for both spin coating and spray pyrolysis.[1] In this study, we included varied concentrations of Al in the optimized β-Ga_2O_3 on n-type silicon and sapphire substrate.

In the $Ga(NO_3)_3$ in NH_4OH, varied concentrations of $Al(NO_3)_3 \cdot 9H_2O$ were added corresponding to 0.6 at% Al, 1.2 at% Al, 2.2 at% Al, and 3.2 at% Al. The mixtures were stirred at 140 °C for 10 h and then cooled to room temperature. The films were deposited by spin coating and spray pyrolysis on sapphire and n-type silicon substrates and postannealed at 930 °C in ambient nitrogen. The films were then characterized and the results were compared.

2.2. Sample Characterization

2.2.1. Identification of Synthesized β-Ga_2O_3:Al

The synthesized films on sapphire were characterized by X-Ray diffraction (XRD) to determine the crystallinity of the formed film structures. The XRD was done using a Bruker D2 Phaser X-Ray diffractometer (XRD) with CuK_α radiation (1.5406 Å), a scanning speed of $0.05° s^{-1}$ for 2θ between 15° and 60° was used, and the diffractograms obtained were compared with JCPDS No.11-370 of gallium oxide.[1]

Raman spectroscopy of the films deposited on n-type silicon was used to determine the vibrational modes of crystals to ascertain the composition of the material present in the sample by analyzing molecular vibrational modes and comparing the results with the functional group data.[20]

2.2.2. Electrical DC Conductivity

The 4-point probe method was used to determine the sheet resistance, R_s, resistivity (ρ), and conductivity (σ) of the thin films.

The sheet resistance was determined using

$$R_S = \frac{\pi}{\ln 2}\frac{\Delta V}{I} \quad (1)$$

and the resistance was determined from the sheet resistance (R_s)

$$\rho = R_s d \quad (2)$$

where d is the film thickness,[4,21] while the conductivity (σ) was determined using

$$\sigma = \frac{1}{\rho} \quad (3)$$

2.2.3. Ohmic and Schottky Contacts and I–V and C–V Characterization

The electron beam evaporator (EBE) was used to make Ohmic and Schottky contacts on β-Ga_2O_3:Al deposited on the n-type silicon substrate (charge carrier concentration of 1.2×10^{14} cm^{-3}). The schematic diagram of EBE employed is illustrated in **Figure 1**.

The average conditions for depositing metal stack contacts were an accelerating voltage of 10 kV and a current of 50 mA, the evaporation rate was kept at 10 Å s^{-1}, and the chamber pressure was initially 6.8×10^{-7} mbar. Metal stack preferences based on previous studies for Ohmic contacts were $Al_2O_5Zn_2$/Ti/Au and $In_{18}O_{28}Sn$/Ti/Au.[14,15,22] But in this study, titanium (Ti), aluminum (Al), nickel (Ni), and gold (Au) were deposited sequentially on the β-Ga_2O_3 film with Ti at the Ga_2O_3 interface, with every metal having its own function. The Ti was preferred for contact with β-Ga_2O_3:Al due to its low work function, and its formation of Ti_2O_3 and Ti_3O_5 with lower work functions than Ti at the interface in forming Ohmic contacts.[15] The second overlayer with a lower work function was Al, which formed an intermetallic compound with Ti to prevent Ti diffusion into Ga_2O_3.

© 2024 The Author(s). physica status solidi (b) basic solid state physics published by Wiley-VCH GmbH

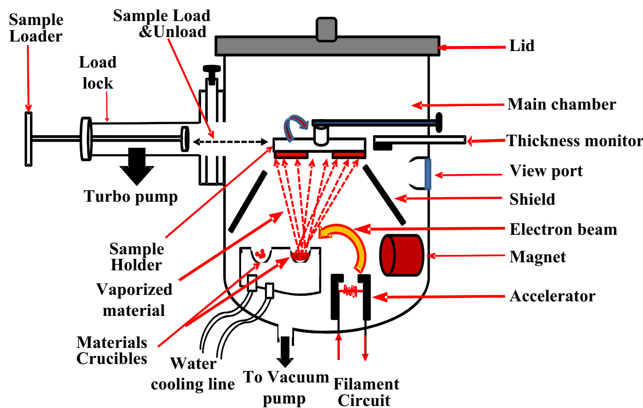

Figure 1. Schematic diagram of EBE.

The third metal layer was Ni (barrier layer) which served the purpose of limiting the indiffusion of the upper protective metal layer (Au) and outer-diffusion of the lower metal layer (Al). The final layer (Au) was the protective layer which reduced oxidation of metal contacts.[18]

Each metal in the stack was deposited to a thickness of 10 nm. The completed stacks were then annealed at 600 °C in nitrogen to increase adhesion between intermetal surfaces, increase oxygen vacancies in the thin films, and hence, reduce the resistance of metal contacts, before depositing the Schottky contacts.[14] The Schottky contacts consisted of palladium (Pd) and gold (Au) deposited to a thickness of 10 nm each. The final sample obtained for *I–V* and *C–V* characterization is illustrated in **Figure 2**.

The metal contacts were analyzed for their suitability in Schottky diode applications from the results of their ideality factor (n), Schottky barrier height (SBH) (ϕ_B), built-in voltage (V_{bi}), saturation current (I_s), series resistance (R_s), and carrier concentration ($N_A - N_D$) that were obtained from the *I–V*, *C–V* analyzer, and satisfied capacitance (C) (Equation (4)).

$$\frac{C}{A} = \sqrt{\frac{\pm q K_s \varepsilon_0 (N_A - N_D)}{2(\pm V_{bi} \pm V - kT/q)}} \tag{4}$$

where K_s is the dielectric constant of the semiconductor, k is the Boltzmann constant, T is temperature, q is a charge, A is diode area, V is applied voltage, ε_0 is the permittivity of free space, N_D is donor impurity concentration, and N_A is accepter impurity concentration.

In Equation (4), the positive sign corresponds to p-type ($N_A > N_D$, $V_{bi} > 0$, and $V > 0$) and the negative sign corresponds to n-type ($N_A < N_D$, $V_{bi} < 0$, and $V < 0$) substrates.[18,21] V is the

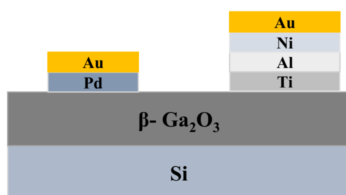

Figure 2. Schematic diagram of Ohmic and Schottky contacts as deposited by EBE.

reverse bias voltage and kT/q accounts for the majority of carrier tail in the space-charge region. The SBH is a function of built-in potential (V_{bi})[19] as in Equation (5)

$$\Phi_B = V_{bi} + V_0 \tag{5}$$

and Equation (6)

$$V_0 = (kT/q)\text{In}(N_c/N_D) \tag{6}$$

where N_c is the effective density of state in the conduction band.[21]

The plot of $1/(C/A)^2$ versus V gives a graph with a slope of $2/[qK_s\varepsilon_0\,(N_A - N_D)]$ and an intercept on V-axis being V_i,[21] where

$$V_i = -V_{bi} + kT/q \tag{7}$$

3. Results and Analysis

3.1. Structural Identification of β-Ga_2O_3:Al

The X-Ray diffractograms (XRD) and Raman spectroscopy analysis of the resulting aluminum-doped β-Ga_2O_3 films using the optimum concentration of the Ga precursors determined previously[1] are discussed as follows. **Figure 3** shows XRD from spin-coated and pyrolytically sprayed Al-doped samples and **Table 1** shows structural parameters obtained to identify the structure of β-Ga_2O_3:Al thin film.

Both spray pyrolysis and spin-coated films' XRD patterns showed typical patterns of β-Ga_2O_3 as confirmed with JCPDS data (No. 11-370). The calculated average crystallite sizes were 19.8 ± 0.2 nm for both spin-coated and pyrolytically sprayed samples. The strain of the films was also determined by applying the Williamson–Hall method,[1] yielding the average strain values of 4.92×10^{-4} and 3.19×10^{-4} for spin-coated and pyrolytically sprayed samples respectively. Doping with Al did not change significantly the crystallite size compared to 17.8 nm for the undoped films. The strain was an order of magnitude less than the undoped films (16.8×10^{-4}), while the crystallinity was enhanced as shown by more symmetric peaks.

Figure 4 shows the Raman spectroscopy results of the aluminum-doped β-Ga_2O_3 films. Five vibrational modes of type Ag and Bg were identified at wavenumbers 375.6, 412.4, 454.9, and 746.7 cm^{-1} for both spin-coated and pyrolytically sprayed samples with only the latter exhibiting additional 444.6 cm^{-1} for the sample with 3.2 at% Al. The peak displacement and intensity signified high order vibrational modes that were enhanced by doping.

As shown in **Table 2**, the results obtained agreed with the LDA data functional group of gallium oxides[23] but with a sizeable margin of shifts compared to undoped β-Ga_2O_3.

The nonmatching 576 cm^{-1} was due to the bending and stretching modes of the sapphire substrate.[1,20,23] The positive shifts demonstrated blue shifts and the negative shifts demonstrated red shifts.

These XRD and Raman shift results confirmed that the doped oxide, as with the undoped oxide, samples still maintained the structural characteristics of the gallium oxide functional group with good stability when exposed to X-Ray radiation and the green laser of Raman.

© 2024 The Author(s). physica status solidi (b) basic solid state physics published by Wiley-VCH GmbH

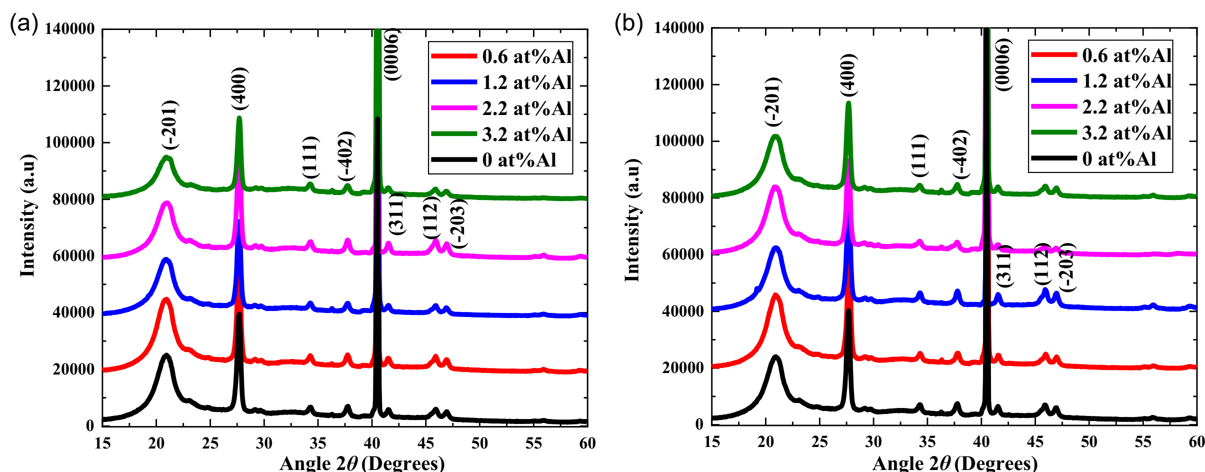

Figure 3. X-Ray diffractograms of β-Ga_2O_3 doped with varied concentrations of Al deposited on sapphire using a) spin coated at room temperature and b) pyrolytically sprayed at 200 °C and postannealed at 930 °C in ambient nitrogen. The peak labeled (0006) is from the sapphire substrate.

Table 1. Average crystallite size (D), strain (ε), and lattice parameters of undoped β-Ga_2O_3 and β-Ga_2O_3:Al films.

Synthesis technique	Spin coated	Pyrolytically sprayed	Undoped β-Ga_2O_3
Average crystallite size [D (nm) $\pm$ 0.2]	19.8	19.8	17.8
Crystallite strain [(ε) $\times 10^{-4}$]	4.92	3.19	16.8
a [nm]	11.97	12.06	12.35
b [nm]	2.96	2.99	3.07
c [nm]	5.71	5.75	5.85
γ [°]	104.05	103.98	103.77

3.2. Electrical Conductivity

Electrical characterization of β-Ga_2O_3:Al was done to determine the viability of doping gallium oxide to make the WBGS appropriate for solar cells application in a photovoltaic cell. In this analysis, resistivity and conductivity of the doped material were considered. This characterization was based on measured quantities of current, voltage, and calculated resistivity of the deposited films.

The resistivities of the doped films are demonstrated in **Figure 5**. The resistivity of the films decreased with the current increase through the thin film. The β-Ga_2O_3 film sample with 2.2 at% Al-doped exhibited the lowest resistivity with the pyrolytically sprayed sample demonstrating lower resistivity compared to the spin-coated ones of the same dopant concentration. Thus, the 2.2 at% Al demonstrated optimal resistivity for a given value of current. The data summary of the electrical properties and film thickness obtained is shown in **Table 3**.

Another aspect of electrical characterization that was considered in this analysis was the conductivity of the doped films. This parameter was calculated based on Equation (1)–(3) and the results of each sample are shown in Table 3. They were compared to the concentration of Al in β-Ga_2O_3 as illustrated in **Figure 6**.

The marked conductivity of n-type silicon used as a substrate in this study is $2.0\,\Omega^{-1}\,\text{cm}^{-1}$. The doped samples showed

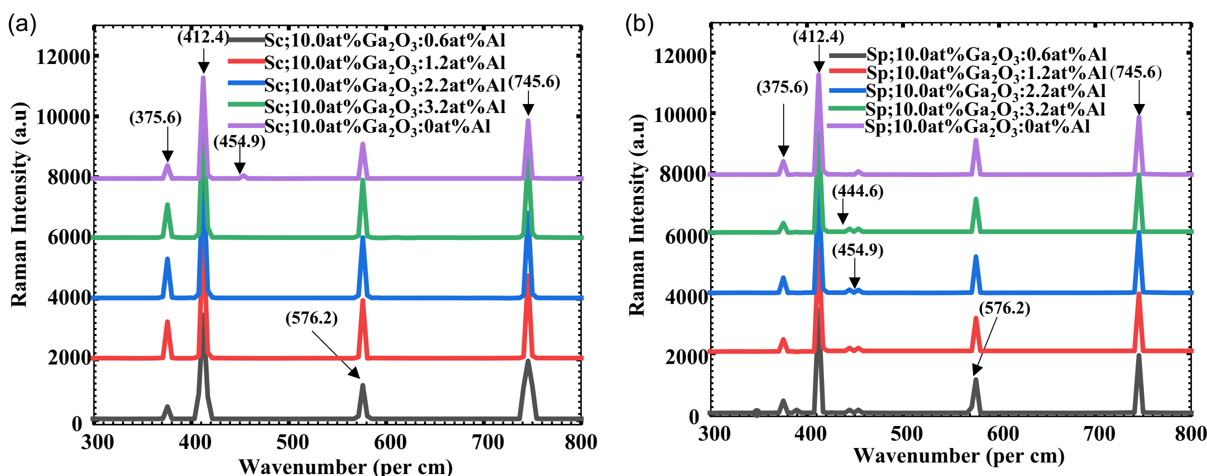

Figure 4. Raman spectroscopy of a) spin-coated and b) pyrolytically sprayed β-Ga_2O_3:Al on sapphire.

© 2024 The Author(s). physica status solidi (b) basic solid state physics published by Wiley-VCH GmbH

Table 2. LDA calculated[20,23] and experimental[20,23] functional groups' data vibrational modes of gallium oxide compared to obtained vibrational modes of β-Ga_2O_3:Al.

SNo	1	2	3	4	5	6	7	8	9	10	11	12	13	14	15	16
Mode symmetry	A_g	B_g	B_g	A_g	A_g	A_g	A_g	B_g	A_g	A_g	B_g	Si	A_g	B_g	A_g	A_g
LDA calculated frequency [cm^{-1}]	104	113	150	160	207	317	348	356	414	469	474	–	601	624	635	732
Experimental data freq. [cm^{-1}]	111	114	147	169	199	318	346	353	415	475	–	–	628	651	657	763
This work freq. [cm^{-1}]	–	–	–	–	–	–	376	412	445	455	–	576	–	–	–	746
Frequency shift [cm^{-1}]	–	–	–	–	–	–	+30	+59	+30	−20	–	–	–	–	–	−17

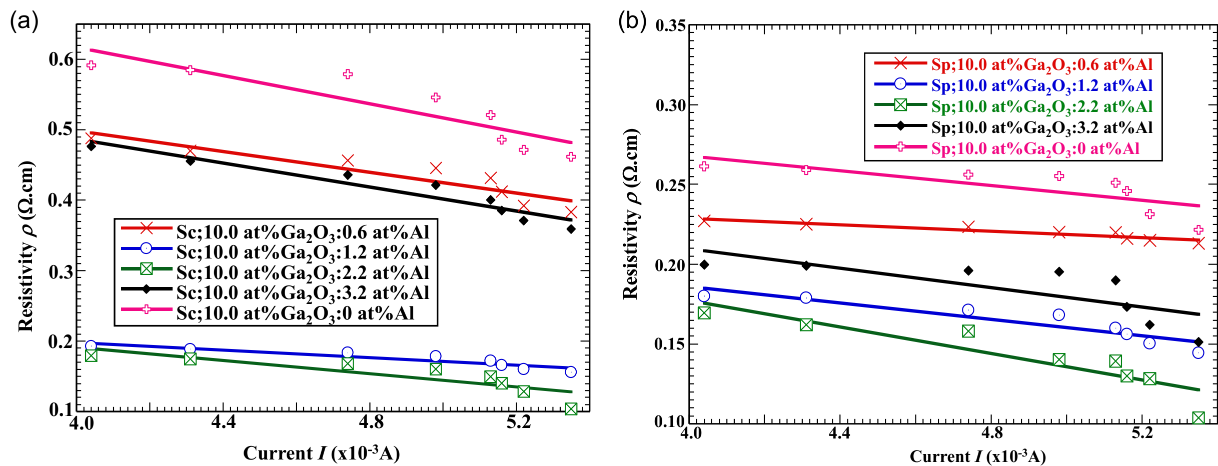

Figure 5. Resistivity versus current of a) spin-coated and b) pyrolytically sprayed β-Ga_2O_3:Al deposited on silicon.

Table 3. Average summary results of electrical data analysis of β-Ga_2O_3:Al for spin-coated (Sc) samples and pyrolytically sprayed (Sp) samples.

Sample	0 at% Al		0.6 at% Al		1.2 at% Al		2.2 at% Al		3.2 at% Al	
Synthesis technique	Sc	Sp	Sc	Sp	Sc	Sp	Sc	Sp	Sc	Sp
Thickness [$d \times 10^2$(nm) $\pm$ 0.05]	2.51	2.53	1.63	1.56	1.66	1.7	2.79	2	2.95	2.3
Resistivity [$\rho_s \times 10^{-1}$ (Ω cm) $\pm$ 0.05]	2.63	2.48	2.32	2.2	1.75	1.64	1.51	1.41	2.26	1.83
Sheet resistance [$R_s \times 10^4$($\Omega/\square$) $\pm$ 0.05]	2.22	0.98	2.67	1.41	1.05	0.96	0.54	0.71	1.40	0.80
Conductivity [σ (Ω^{-1} cm^{-1}) $\pm$ 0.05]	3.80	4.03	4.30	4.55	5.71	6.10	6.62	7.09	4.42	5.46

conductivity greater than that of n-type silicon substrate and varied as the dopant concentration changed. This demonstrated that the varied conductivity obtained in this study was predominantly from the deposited film of Al-doped β-Ga_2O_3.

From the illustration of Figure 6, the pyrolytically sprayed films had better conductivity than spin-coated films for equal dopant concentration. In all samples, the doped samples had better conductivity than the undoped samples. This could have been enhanced by increased crystallinity and less strain on the structure. As the lattice-free volume increases, the lattice spacing increases and the ion mobility increases; therefore, ionic conductivity increases.[12,24] Higher-order vibrational modes caused by doping of samples, that are displayed by Raman spectroscopy, could also have enhanced conductivity.[12,24]

Based on the electrical property summary results in Table 3, the electrical property of the Al-doped β-Ga_2O_3 improves with increased dopant concentration, but at some point, there is a decline in the same as dopant concentration is increased. This led to the optimal dopant concentration obtained at 2.2 at% Al. This could be attributed to the annealing of the samples at higher temperatures of 930 °C in nitrogen ambient that may have created more oxygen vacancies in the β-Ga_2O_3.[25] Once the saturation point of dopant is reached, any further doping creates less oxygen vacancies. At the same time, higher concentrations of charge carriers cause traffic jam of charges, and therefore, this causes immobility of charge carriers. These two factors lead to less conductivity of the doped material.

3.3. Metal Contacts Analysis

Wide bandgap semiconductors are becoming more viable for electronic applications. For applications in the making of transistors and diodes, metal contacts for β-Ga_2O_3:Al were deposited in an EBE. *I*–*V* and *C*–*V* analysis was done with Ohmic contact

© 2024 The Author(s). physica status solidi (b) basic solid state physics published by Wiley-VCH GmbH

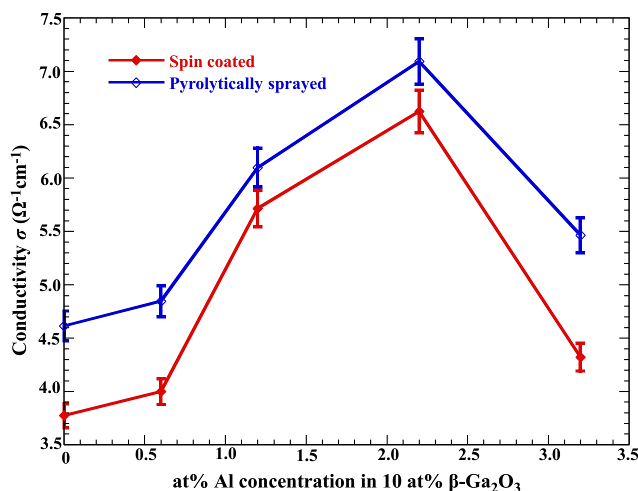

Figure 6. Conductivity versus Al concentration in spin-coated and pyrolytically sprayed β-Ga_2O_3:Al films deposited on n-type silicon.

metal stacks of Ti/Al/Ni/Au and Schottky contact metal stacks of Pd/Au.

Analytical graphs for *I–V* characterization of electrode contacts, obtained from the *I–V* analysis of spin-coated and pyrolytically sprayed β-Ga_2O_3:Al, are shown in **Figure 7**. The curves depict the typical curves for Schottky diodes with generally more than one order of magnitude difference between the forward and reverse current at 2 and −2 V, respectively.

The summary of the electrical properties obtained from the analysis of the *I–V* curves of spin-coated and pyrolytically sprayed β-Ga_2O_3:Al is tabulated in **Table 4**.

In both spin-coated and pyrolytically sprayed β-Ga_2O_3:Al, the addition of 2.2 at% Al gave the best properties of Ga_2O_3:Al with metal stacks of Ti/Al/Ni/Au for Ohmic contacts and Pd/Au for Schottky contacts compared to earlier stacks so far reported.[14] The table demonstrates the 2.2 at% Al as an optimal concentration that forms the best Schottky diodes with the lowest ideality factors, highest SBH, and lowest saturation current in the range measured.

3.4. *C–V* Characterization of β-Ga_2O_3:Al Electrode Contacts

This characterization is necessary for determining the viability of WBGS for lower energy loss when applied in making diodes. In this study, *C–V* characterization of metal contacts of β-Ga_2O_3:Al was carried out and the results obtained were plotted as illustrated in **Figure 8**.

The $1/C^2$ versus V is linear with a slope representing $2/[qK_s\varepsilon_0(N_A - N_D)]$ as demonstrated in Equation (4). This is an indication of good Ohmic and Schottky contacts for an ideal transistor application. The summary of electrical properties obtained from these graphs is tabulated in **Table 5**.

From the results, the concentration of 2.2 at% Al can be considered as optimal for β-Ga_2O_3:Al that responded best to metal contacts with the lowest built-in voltage, highest SBH, and highest carrier concentration. Compared to previous studies, these

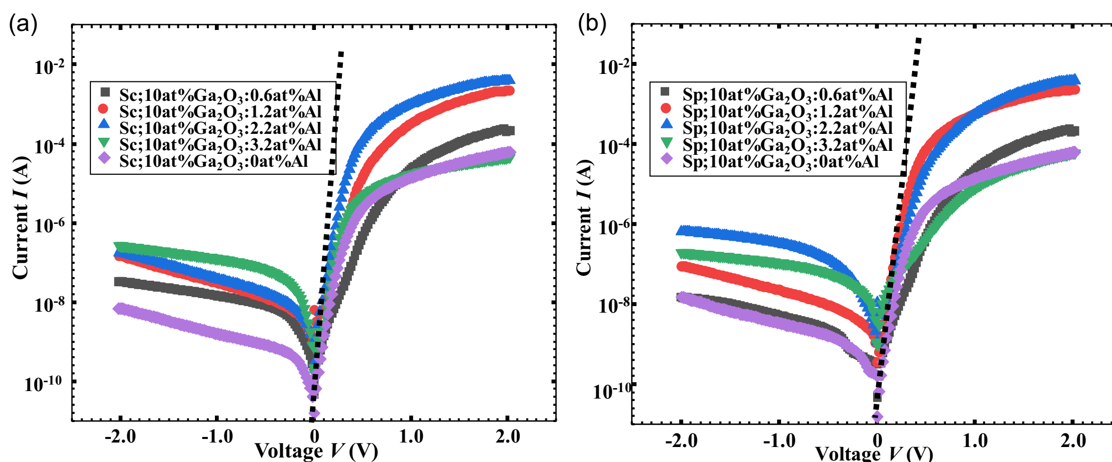

Figure 7. Logarithmic *I–V* characterization of a) spin-coated and b) pyrolytically sprayed samples of β-Ga_2O_3:Al at varied concentrations of Al.

Table 4. *I–V* properties for spin-coated (Sc) and pyrolytically sprayed (Sp) β-Ga_2O_3:Al deposited on an n-type silicon substrate.

Dopant concentration	0.0 at% Al		0.6 at% Al		1.2 at% Al		2.2 at% Al		3.2 at% Al	
Deposition technique	Sc	Sp	Sc	Sp	Sc	Sp	Sc	Sp	Sc	Sp
Ideality factor [n]	1.238	1.134	1.132	1.130	1.112	1.105	1.099	1.094	1.129	1.127
Saturation current [$I_s \times 10^{-6}$ (A)]	5.19	5.09	3.840	3.739	3.203	3.193	3.170	3.102	3.506	3.479
SBH [eV]	0.594	0.597	0.652	0.658	0.688	0.704	0.731	0.877	0.659	0.675
Series resistance [R_s (Ω)]	537.3	596.7	747.2	751.6	896.4	901.7	948.3	954.6	806.6	877.8

© 2024 The Author(s). physica status solidi (b) basic solid state physics published by Wiley-VCH GmbH

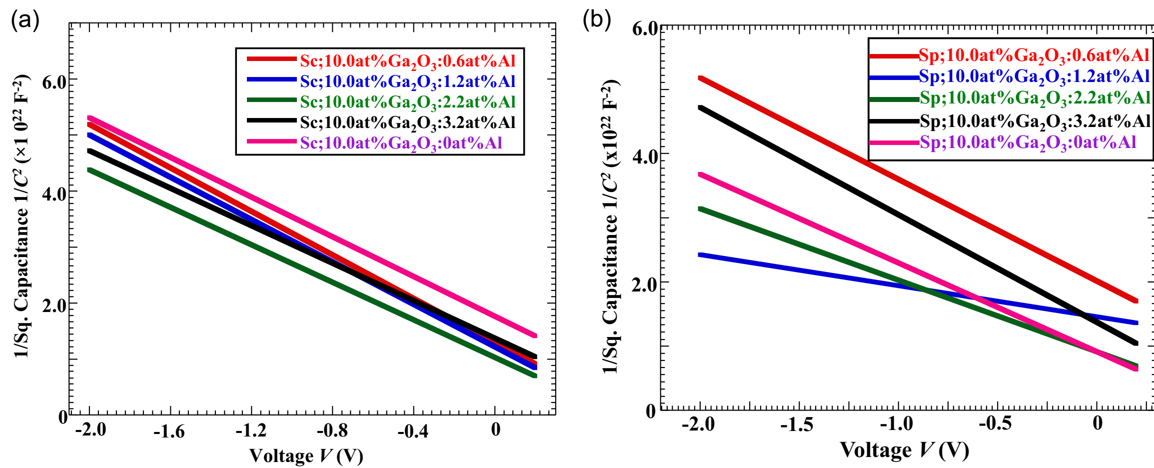

Figure 8. $1/C^2$–V characterization of a) spin-coated and b) pyrolytically sprayed samples of β-Ga_2O_3:Al with the ratios of 10.0 at%Ga_2O_3 to varied concentrations of Al.

Table 5. C–V properties for spin-coated (Sc) and pyrolytically sprayed (Sp) β-Ga_2O_3:Al deposited on n-type silicon substrate.

Dopant concentration	0.0 at% Al		0.6 at% Al		1.2 at% Al		2.2 at% Al		3.2 at% Al	
Deposition technique	Sc	Sp	Sc	Sp	Sc	Sp	Sc	Sp	Sc	Sp
Built-in voltage [V_{bi} (eV)]	0.86	0.77	0.86	0.58	0.71	0.44	0.57	0.35	0.73	0.52
SBH [eV]	1.18	1.20	1.33	1.35	1.58	1.64	1.78	1.89	1.39	1.42
Carrier concentration [$N_A - N_D \times 10^{16}$ (cm^{-3})]	0.28	0.39	1.05	1.13	1.39	1.78	1.61	1.87	1.06	1.33

results are within the expected ideal quantities of the ideal diode.[5]

From the I–V summary table, pyrolytically sprayed sample films demonstrated better diode properties, that is, lower n, lower I_s, higher R_s, and higher SBH, compared to spin-coated samples. Variations were, however, minimal, an indication of close similarity in deposition techniques. Similarly, from the C–V summary table, pyrolytically sprayed sample films showed lower V_{bi} and higher carrier concentration compared to spin-coated sample films, with very small deviations. The choice of metal stacks for and sequence of deposition for the formation of electrode contacts is crucial to note. Ambient of annealing, in this case nitrogen, and annealing temperatures determined the formation of oxygen vacancies that greatly improved the electrical conductivity of β-Ga_2O_3:Al.[14]

4. Summary

In this study, a novelty precursor of tetrahydroxogallate (III) ammonium was applied in synthesizing samples of β-Ga_2O_3 by either spin coating or spray pyrolysis. The thin films of the samples made were first structurally characterized by XRD and Raman spectroscopy. This confirmed the thin films to be polycrystalline nanoparticles of β-Ga_2O_3:Al.

Sprayed samples with precursor dopant concentrations of 1.2 at% Al, and 2.2 at% Al demonstrated slightly higher conductivities compared to spin-coated samples. Metal contacts deposited on 2.2 at% Al of pyrolytically sprayed films demonstrated better electrical properties with ideality factor of 1.09 and I–V SBH of 0.88 eV compared to 0.73 eV exhibited by the spin-coated film with an ideality factor of 1.1. Built-in voltage (V_{bi}) of 0.35 eV and 0.57 eV were also reported for pyrolytically sprayed and spin-coated samples, respectively, with saturation current (I_s) of 3.10×10^{-6} and 3.17×10^{-6} A. These characterization properties placed 2.2 at% Al precursor concentration as the optimal concentration of this study with metal stacks of Ti/Al/Ni/Au for Ohmic contacts and Pd/Au for Schottky contacts for the diode electrodes compared to earlier stacks so far reported in the literature. The combination of metal stacks, Ti/Al/Ni/Au for Ohmic contacts and Pd/Au for Schottky contacts, and sequence of deposition for the formation of electrode contacts have not been used before on β-Ga_2O_3:Al and have resulted in improved electrical properties. Ambient annealing in nitrogen at 930 °C is speculated to result in the formation of oxygen vacancies that greatly influenced the improved electrical conductivity.[14]

5. Conclusion

The aim of this study was to optimize the dopant concentration in the synthesis of β-Ga_2O_3:Al thin films and investigate metal stacks that can adequately make electrode contacts with minimum resistance at contact points of the diode, hence making the β-Ga_2O_3:Al diode more efficient. In this study, tetrahydroxogallate (III) ammonium was originally applied in synthesizing β-Ga_2O_3. Comparison of two less costly synthesis techniques (spin coating and spray pyrolysis) was investigated and they were

© 2024 The Author(s). physica status solidi (b) basic solid state physics published by Wiley-VCH GmbH

found to have similar results with very minimal deviations. The purpose of Al dopant in this study was to modify the structure and the electrical properties of the β-Ga_2O_3 as this created more oxygen vacancies and especially at higher postannealing temperatures with enhanced crystallinity and increased conductivity of the β-Ga_2O_3 thin films. The 2.2 at% Al optimal dopant concentration is of great significance for future research in this field of study as it will form the basis for making ideal β-Ga_2O_3:Al diodes for applications in high-power electronics with thermal stability. The novel four metal stack contacts enhanced the electrical properties of the β-Ga_2O_3:Al diodes.

Acknowledgements

The authors would like to thank the South African National Research Foundation (NRF) for financial support during this study under grant nos. 111744 and 137977, the Technical University of Mombasa, and the University of Pretoria.

Conflict of Interest

The authors declare no conflict of interest.

Author Contributions

Valentine W. Muramba: Conceptualization, Methodology, Investigation, Analysis, Writing—original draft. **Abdulraoof I. A. Ali**: Methodology, Investigation, Analysis, Manuscript corrections. **Jacqueline M. Nel**: Investigation, Writing—review and editing, Supervision, Project administration, Funding acquisition.

Data Availability Statement

Research data are not shared.

Keywords

β-Ga_2O_3, capacitance–voltage, current–voltage, doping, metal stacks, Schottky barriers

Received: August 14, 2024
Revised: September 26, 2024
Published online:

[1] V. W. Muramba, A. I. Ali, J. M. Nel, *J. Mater. Sci. Mater. Electron.* **2023**, *34*, 2221.
[2] Y. Jae-Hyuck, R. Subrina, A. Lange, H. Zhao, E. Selim, *Appl. Phys. Lett. Mater.* **2018**, *6*, 036105.
[3] S. J. Pearton, J. Yang, P. H. Cary, R. Fangfang, J. Kim, M. J. Tadjer, M. A. Mastro, *Appl. Phys. Rev.* **2018**, *5*, 011301.
[4] J. D. Cutnell, K. W. Johnson, in *Physics*, 5th ed., John Wiley & Sons Inc, New York **2001**.
[5] M. Xiaofan, Z. Yuming, D. Linpeng, J. Renxu, *Results Phys.* **2017**, *7*, 1582.
[6] P. Mandal, R. Sudesna, U. P. Singh, *Optical and Quantum Electronics* **2022**, *54*, 476.
[7] K. Sunjae, R. Heejoong, L. In-Gyu, S. Myunghun, J. C. Byung, S. H. Wan, *RSC Adv.* **2021**, *11*, 7338.
[8] K. Sunjae, R. Heejoong, L. In-Gyu, M. Jeonghyun, S. H. Wan, *J. Alloys Compd.* **2022**, *931*, 167502.
[9] T. Xiao, H. L. Kuang, H. L. Che, M. T. V. Jose, W. Chuaju, N. Xiao, L. Xiaohang, *J. Eur. Ceram. Soc.* **2022**, *42*, 175.
[10] V. D. Luang, N. A. Nguyen, B. T. Tran, L. D. Chung, Q. H. Nguyen, D. T. Nhung, T. P. Mai, N. M. Phan, D. P. Doan, V. T. Pham, *J. Diam. Relat. Mater.* **2020**, *108*, 107980.
[11] L. Pengkun, H. Xueli, C. Duanyang, S. Qinglin, Q. Hongji, *J. Alloys Compd.* **2022**, *933*, 167802.
[12] K. Belova, A. Egorova, S. Pachina, I. Animitsa, *J. Appl. Sci.* **2022**, *12*, 1181.
[13] P. R. Jubu, F. K. Yam, O. S. Obaseki, Y. Yusof, *J. Mater. Sci. Semicond. Process.* **2021**, *121*, 105361.
[14] Y.-W. Huan, S.-M. Sun, C.-J. Gu, W.-J. Liu, S.-J. Ding, H.-Y. Yu, C.-T. Xia, D. W. Zhang, *Nanoscale Res. Lett.* **2018**, *13*, 246.
[15] E. Farzana, Z. Zg, K. P. Pran, R. A. Arehart, S. A. Ringel, *Appl. Phys. Lett.* **2017**, *110*, 202102.
[16] D. Linpeng, Z. Shun, P. Kaiwen, Y. Chen, X. Bin, B. Peng, L. Weiguo, *J. Appl. Surf. Sci.* **2021**, *564*, 150386.
[17] N. S. Shivani, K. Mashesh, K. Mukesh, *J. Surf. Interfaces* **2024**, *46*, 103937.
[18] E. Chikoidize, F. Adel, P. T. Amador, Guillaume Sr., T. Tamar, T. T. Coung, T. H. Tung, P. Matthew, S. Russel, M. Jennings, B. Bruno, F. Jomard, D. Yves, *Mater. Today Phys.* **2017**, *3*, 118.
[19] S. M. Sze, K. K. Ng, in *Physics of Semiconductor Devices*, 3rd ed., John Wiley & Sons, Hoboken, NJ **2006**.
[20] S. Kumar, G. Sarau, C. Tessarek, M. Y. Bashouti, A. Hähnel, S. Christiansen, R. Singh, *J. Phys. D* **2014**, *47*, 435101.
[21] D. Schroder, in *Semiconductor Material and Service Characterization*, 3rd ed., John Wiley & Sons, Hoboken, NJ **2006**.
[22] J.-Y. Jung, W.-S. Cho, J.-H. Kim, K.-T. Hwang, E.-T. Kang, K.-S. Han, *Ceram. Int.* **2016**, *42*, 2582.
[23] R. Rahul, *Raman Spectroscopic Evidence for Anharmonic Phonon Lifetimes and Blueshifts in 1d Structures*, Clemson University, Tiger Prints; Condensed Matter Physics Commons. All Dissertations, 73, **2007**, https://tigerprints.clemson.edu/all_dissertations/73 (accessed: May, 2007).
[24] B. Arias, N. Nedev, S. Ghose, J. R. R. Salvador, D. Mateos, M. A. Curiel, O. Pérez, M. Suárez, B. Valdez-Salas, R. Droopad, *Adv. Mater. Sci. Eng.* **2018**, 9450157.
[25] G. Yangyang, L. Ang, F. Qian, H. Zhuangzhuang, F. Zhaoqing, Z. Ke, L. Xiaoli, Z. Chunfu, Z. Hong, M. Wenxiang, J. Zhitai, Z. Jincheng, H. Yue, *Nanoscale Res. Lett.* **2019**,*14*, 2849.

© 2024 The Author(s). physica status solidi (b) basic solid state physics published by Wiley-VCH GmbH